Int. J. Solids Structures Vol. 15, pp. 701–713
Pergamon Press Ltd., 1979. Printed in Great Britain

INTERFACIAL STRESSES IN VISCOELASTIC ADHESIVE-LAYERS DUE TO MOISTURE SORPTION

Y. WEITSMAN
Mechanics and Materials Research Center, Texas A&M University, College Station, TX 77843, U.S.A.

(*Received* 30 *August* 1978; *revised* 15 *December* 1978)

Abstract—This paper concerns the mechanical behavior of an epoxy adhesive layer that is located between stiff adherends as the adhesive absorbs moisture from the ambient environment.

As the moisture penetrates the layer by an extremely slow diffusion process the eposy undergoes a simultaneous process of stress-relaxation. Calculations of viscoelastic interfacial stresses were performed for a time-dependent response which is typical of epoxy for a layer geometry as encountered in practice.

The results show that for exposure to steady ambient humidity the viscoelastic stresses are smaller than their elastic counterparts. However, under fluctuating ambient humidity the viscoelastic response may cause stress reversals, and thereby failure modes, which are not predicted by elasticity theory.

1. INTRODUCTION

Adhesive bonding forms an attractive method of joining structural members. In analyzing the stresses which develop within the bond it is necessary to account for the fact that the adhesive materials respond in a viscoelastic manner under loads and their time-dependent behavior is greatly affected by moisture and temperature.

When two adherends are joined together by a thin adhesive layer the adhesive absorbs moisture from the ambient environment, at its exposed edges, which induces swelling strains into the layer. Since the adherends are much stiffer than the adhesive they constrain the adhesive-layer against its tendency to swell, thus causing the formation of extremely high stresses within the layer. In this paper attention is focused on the interfacial-stresses which arise at the interfaces between the adherends and the adhesive.

Since the moisture penetrates the layer by an extremely slow diffusion process, the epoxy may undergo noticeable creep and relaxation while the diffusion process is in progress. The main purpose of this paper is to relate the interaction, which occurs concurrently, between the two time-dependent phenomena—moisture-diffusion and stress-relaxation.

The analysis employs a variational method and is inherently approximate in nature. It is due to this approximation that the edge singularity in the stress field is replaced here by finite, though large, values. However, for the exceedingly thin layers that are utilized in practice, the selected expressions for the displacement fields should provide a good approximation. Furthermore, the approximation should not detract from the basic purpose of this work which is to provide information about the relative influence of the diffusion and relaxation times.

2. FORMULATION

Consider a semi-infinite, isotropic and elastic adhesive layer, of thickness $2a$, between two semi-infinite adherend plates as shown in Fig. 1.

Let X, Y denote Cartesian coordinates and t time. Let $\varepsilon(X, t)$ represent the unconstrained swelling induced by moisture and μ, ν be the elastic-shear-modulus and Poisson's ratio, respectively. Assume a state of plane-strain.

Introduce the following non-dimensional quantities

$$x = X/a,\ y = Y/a,\ e(x,t) = \varepsilon(X/a, t)$$
$$s_x = \sigma_x/\mu,\ s_y = \sigma_y\,\mu,\ s_{xy} = \tau_{xy}/\mu. \tag{1}$$

Also, denote

$$f_1 = 2\nu/(1-2\nu),\quad f_2 = 2(1-\nu)/(1-2\nu),\quad f_3 = 2(1+\nu)/(1-2\nu).$$

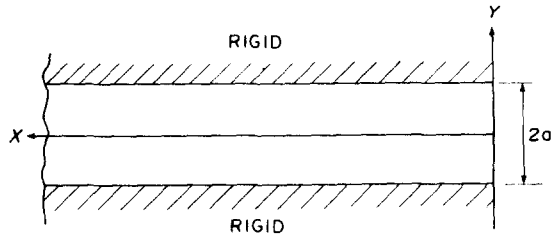

Fig. 1. The adhesive layer between rigid adherends exposed to moisture at $X = 0$.

Consider now the following, approximate, form for the displacement fields within the adhesive-layer

$$\begin{aligned} U(X, Y) &= a u_0(x) + \frac{1}{2} a\, u_2(x) y^2 \\ V(X, Y) &= a\, v_1(x) y + \frac{1}{3} a\, v_3(x) y^3. \end{aligned} \tag{2}$$

In (2) U and V are components of displacement in the X and Y directions, respectively, and u_0, u_2, v_1, v_3 are dimensionless, yet to be determined functions of the dimensionless coordinate x. Note that for an induced swelling-strain of the form $e(x, t)$ the displacements U and V possess the required symmetries in Y.

Form (2) is the lowest-order approximation which provides information on the interfacial stresses, at the boundary between adhesive and adherend, in a self-contained manner. For exceedingly thin layers the approximation should provide sufficient accuracy.

Expressions (2) are essentially the same as used in Ref. [1].

Employing Hooke's law we obtain the following non-dimensional form for stress–strain relations:

$$\begin{bmatrix} s_x \\ s_y \\ s_{xy} \end{bmatrix} = \begin{bmatrix} f_2 & f_1 & f_3 & 0 \\ f_1 & f_2 & f_3 & 0 \\ 0 & 0 & 0 & 1 \end{bmatrix} \begin{bmatrix} u_0' + \frac{1}{2} u_2' y^2 \\ v_1 + v_3 y^2 \\ -e \\ u_2 y + v_1' y + \frac{1}{3} v_3' y^3 \end{bmatrix} \tag{3}$$

where primes designate derivatives with respect to x.

In addition, due to the assumed rigidity and immobility of the adherends we have the following boundary conditions:

$$\begin{aligned} u(x, 1, t) &= 0 \\ v(x, 1, t) &= 0. \end{aligned} \tag{4}$$

In view of the constraints implied by boundary conditions (4) it is obvious that, when employing a variational formulation, the unknown functions u_0, u_2, v_1, and v_3 in (2) cannot be varied independently. As noted in [1] the four above mentioned functions can be treated independently of each other by introducing suitable Lagrange multipliers s_n and s_t. It turns out that s_n and s_t, which are the dimensionless force-conjugates of $v(x, 1, t)$ and $u(x, 1, t)$ respectively, represent the sought after interfacial normal and shear stresses.

Employment of the principle of virtual work, and utilization of the Lagrange multipliers in analogy with [1],† yields the following expression for the variation of the internal energy δE

†See particularly the section Variational Formulation of the Totally Constrained Case ($v_0 = 0$).

$$\delta E = \mu a^2 \int_0^\infty \left\{ \int_0^1 \left[s_x \left(\delta u_o' + \frac{1}{2} y^2 \delta u_2' \right) + s_y (\delta v_1 + y^2 \delta v_3) + s_{xy} \left(y \delta u_2 + y \delta v_1' + \frac{1}{3} y^3 \delta v_3' \right) \right] dy \right.$$

$$\left. - s_t \left(\delta u_0 + \frac{1}{2} \delta u_2 \right) - \delta s_t \left(u_0 + \frac{1}{2} u_2 \right) - s_n \left(\delta v_1 + \frac{1}{3} \delta v_3 \right) - \delta s_n \left(v_1 + \frac{1}{3} v_3 \right) \right\} dx. \quad (5)$$

Similarly, the variation of the external work, δW, is given by

$$\delta W = \mu a^2 \int_0^1 \left[s_x^*(0, y) \left(\delta u_0 + \frac{1}{2} y^2 \delta u_2 \right) + s_{xy}^*(0, y) \left(y \delta v_1 + \frac{1}{3} y^3 \delta v_3 \right) \right] dy. \quad (6)$$

Integration by parts of (5) and employment of (3) yield, upon factoring out the now independent variations δu_0, δu_2, δv_1 and δv_3:

$$\begin{aligned}
&\frac{2}{3} f_2 u_0'' - f_3 e' + s_t = 0 \\
&\frac{1}{15} f_2 u_0'' - \frac{2}{15} (f_1 + 1) v_1' + \frac{2}{3} u_0 - \frac{1}{6} f_3 e' + \frac{1}{2} s_t = 0 \\
&\frac{2}{3} (f_1 + 1) u_0' - \frac{2}{15} v_1'' - f_3 e - s_n = 0 \\
&\frac{2}{5} (f_1 + 1) u_0' - \frac{2}{35} v_1'' - \frac{4}{5} f_2 v_1 - f_3 e - s_n = 0.
\end{aligned} \quad (7)$$

To these are adjoined the constraint conditions

$$\begin{aligned}
u_0 + \frac{1}{2} u_2 = 0 \\
v_1 + \frac{1}{3} v_3 = 0.
\end{aligned} \quad (8)$$

Equations (7) and (8) express the field equations of the problem. The concomitant from the integration-by-parts of (5) combines with (6) to determine the boundary conditions at $x = 0$. This combination, together with (3), yields

$$\begin{aligned}
-7 u_0 + 2 v_1' = 0 \\
2 u_0' + \frac{f_1}{f_2} v_1 = \frac{5}{2} \frac{f_3}{f_2} e(0, t).
\end{aligned} \quad (9)$$

Note that the boundary conditions (9) were obtained after employment of (8), which hold also at $x = 0$.

In order to solve for u_0 and v_1 we first eliminate s_t between the first pair of (7) and s_n between the last pair. Next, we employ (8) to eliminate u_2 and v_3. This procedure yields:

$$\begin{aligned}
2 f_2 u_0'' + (f_1 + 1) v_1' - 5 u_0 = \frac{5}{2} f_3 e' \\
\frac{2}{7} v_1'' - (f_1 + 1) v_0' - 3 f_2 v_1 = 0.
\end{aligned} \quad (10)$$

The solution of (10) is expressed with the aid of the following second order equation

$$\frac{4}{7} f_2 Z^2 + \left[(f_1 + 1)^2 - 6 f_2^2 - \frac{10}{7} \right] Z + 15 f_2 = 0. \quad (11)$$

Denote the roots of (11) by Z_1 and Z_2 and define

$$\alpha_1 = \sqrt{Z_1}, \quad \alpha_2 = \sqrt{Z_2}$$

$$\chi_{1,2} = \frac{(f_1+1)\alpha_{1,2}}{(2/7)Z_{1,2} - 3f_2} \qquad D = \frac{5}{4}\frac{f_3}{f_2}\frac{1}{\alpha_1\chi_2 - \alpha_2\chi_1}.$$

The solution of (10), which vanishes as $x \to \infty$, is

$$u_0 = D\left[\chi_1 \int_x^\infty \sinh \alpha_2(x-s)e'(s)\,ds - \chi_2 \int_x^\infty \sinh \alpha_1(x-s)e'(s)\,ds\right] + A_1 e^{-\alpha_1 x} + A_2 e^{-\alpha_2 x}$$

$$v_1 = D\chi_1\chi_2 \int_x^\infty \left[\cosh \alpha_2(x-s) - \cosh \alpha_1(x-s)\right] e'(s)\,ds - \chi_1 A_1 e^{-\alpha_1 x} - \chi_2 A_2 e^{-\alpha_2 x}. \tag{12}$$

In (12) A_1 and A_2 are arbitrary constants that are determined with the aid of boundary conditions (9).

3. ELASTIC SOLUTION FOR MOISTURE DIFFUSION UNDER CONSTANT AMBIENT HUMIDITY

It has been observed [2], [3]† that the saturation-moisture level in "neat" epoxy, as well as in epoxy-based composites, depends on the relative humidity of the ambient environment. The dilatational strains that accompany moisture sorption are about 2/3 of the swelling that would be anticipated by straightforward "volume additivity".

The penetration of moistures into several epoxy resins was shown to follow the classical diffusion equations [2–4].

For the one-dimensional diffusion process considered herein, it follows that under constant ambient humidity the moisture-induced swelling is given by

$$\varepsilon(X, t) = A \operatorname{erfc}\left(\frac{X}{2\sqrt{kt}}\right). \tag{13}$$

In (13) A is a constant which converts moisture content to dilatational strain and k is the coefficient of moisture diffusion.

Introduce the non-dimensional time $\beta = kt/a^2$, then the non-dimensional version of (13) reads

$$e(x, \beta) = A \operatorname{erfc}(x/2\sqrt{\beta}). \tag{14}$$

Substitution of (14) into (12) leads to a closed-form solution for all the integrals therein [5, 6], e.g.

$$\int_x^\infty \sinh \alpha(x-s)e'(s)\,ds = -\frac{A}{2}e^{\beta\alpha^2}\left\{\sinh \alpha x\left[1 - \frac{1}{2}\left(\operatorname{erf}\left(\frac{x}{2\sqrt{\beta}} + \alpha\sqrt{\beta}\right)\right.\right.\right.$$

$$\left.\left.\left. - \operatorname{erf}\left(\frac{x}{2\sqrt{\beta}} - \alpha\sqrt{\beta}\right)\right)\right] - \frac{1}{2}\cosh \alpha x\left[\operatorname{erf}\left(\frac{x}{2\sqrt{\beta}} + \alpha\sqrt{\beta}\right) - \operatorname{erf}\left(\frac{x}{2\sqrt{\beta}} - \alpha\sqrt{\beta}\right)\right]\right\}$$

and a similar expression for

$$\int_x^\infty \cosh \alpha(x-s)e'(s)\,ds.$$

With the simpler, closed-form version of u_0 and v_1 that replaces all the integrals in (12) it is possible to evaluate analytically the unknowns A_1 and A_2 therein.

†For most of this information, the author is greatly indebted to Messrs. J. E. Halkias and E. L. McKague of General Dynamics Corporation, Fort Worth Division.

Employing the boundary conditions (9), with $e(0, t) = A$, the values of A_1 and A_2 are determined from the following two-by-two algebraic system:

$$\begin{bmatrix} L_1 & L_2 \\ M_1 & M_2 \end{bmatrix} \begin{bmatrix} A_1 \\ A_2 \end{bmatrix} = \begin{bmatrix} D(-L_2\chi_1 J_2 + L_1\chi_2 J_1) \\ -\frac{5}{2}\frac{f_3}{f_2}A + D(-M_1\chi_2 K_1 + M_2\chi_1 K_2) \end{bmatrix} \tag{15}$$

where, in (15)

$$L_{1,2} = 7 - (2\alpha\chi)_{1,2} \qquad M_{1,2} = \left(2\alpha + \frac{f_1}{f_2}\chi\right)_{1,2}$$

$$K_{1,2} = -A\, e^{\beta\alpha_{1,2}^2} \qquad J_{1,2} = -K_{1,2}\,\mathrm{erf}(\alpha_{1,2}\sqrt{\beta}).$$

Solving for A_1 and A_2 from (15) we obtain the complete solution to u_0 and v_1 in (12). This, in turn, enables us to evaluate the interfacial tractions s_n and s_t by using the first and third of eqns (7).

After straightforward, though tedious, manipulations we obtain

$$\begin{aligned} s_n(x,\beta) &= \frac{2}{3}D\,[\alpha_2\chi_1 P_2 K_2(x,\beta) - \alpha_1\chi_2 P_1 K_1(x,\beta)] \\ &\quad -\frac{2}{3}\alpha_1 P_1 A_1\, e^{-\alpha_1 x} - \frac{2}{3}\alpha_2 P_2 A_2\, e^{-\alpha_2 x} - f_3\, e(x,\beta) \\ s_t(x,\beta) &= -\frac{2}{3}f_2 D[\alpha_2^2\chi_1 J_2(x,\beta) - \alpha_1^2\chi_2 J_1(x,\beta)] \\ &\quad -\frac{2}{3}f_2(\alpha_1^2 A_1\, e^{-\alpha_1 x} + \alpha_2^2 A_2\, e^{-\alpha_2 x}) - \frac{Af_3}{6\sqrt{\pi\beta}}\, e^{-(x^2/4\beta)}. \end{aligned} \tag{16}$$

In (16)

$$J_{1,2}(x,\beta) = -\frac{A}{2}\, e^{\beta\alpha_{1,2}^2}(\psi_{1,2}^+ - \psi_{1,2}^-)$$

$$K_{1,2}(x,\beta) = -\frac{A}{2}\, e^{\beta\alpha_{1,2}^2}(\psi_{1,2}^+ + \psi_{1,2}^-)$$

where

$$\psi_{1,2}^+ = e^{\alpha_{1,2}x}\,\mathrm{erfc}(\alpha_{1,2}\sqrt{\beta} + x/2\sqrt{\beta})$$

$$\psi_{1,2}^- = e^{-\alpha_{1,2}x}\,\mathrm{erfc}\,(-\alpha_{1,2}\sqrt{\beta} + x/2\sqrt{\beta}).$$

Also,

$$P_{1,2} = f_1 + 1 - \frac{1}{5}(\alpha\chi)_{1,2}.$$

Form (16) is the elastic solution to the present problem. While this form provides a necessary step toward the generation of the viscoelastic solution, because its Laplace transform is readily available, it cannot be evaluated numerically for a wide range of x and t because $J_1(x, \beta)$, $K_1(x, \beta)$, A_1 and A_2 become numerically unstable.† Difficulties of this sort stem from the peculiar geometry of the adhesive layer, namely, the extremely small ratio of thickness to length.

†For $x = 3$ and $t = 1000$, with typical values for k, a and ν, J_1 and K_1 involve products of numbers of $0(10^{22})$ with numbers of $0(10^{-22})$, thus exceeding the accuracy provided even by "double precision".

The difficulty is overcome by the employment of an approximate form of erfc (z), as follows[7]:

$$\operatorname{erfc} z = Q(t(z))\,e^{-z^2} \tag{17}$$

where

$$Q(t) = \sum_{j=1}^{5} a_j t^j \text{ and } t(z) = (1+pz)^{-1}\ddagger.$$

Appropriate substitution of (17) into (16) yields an alternative, numerically stable, form for the interfacial stresses. We obtain

$$\begin{aligned}
\frac{1}{A}s_n(x,\beta) &= \frac{5}{3}\frac{f_3}{f_2}\frac{\alpha_2 P_2 L_1 e^{-\alpha_2 x} - \alpha_1 P_1 L_2 e^{-\alpha_1 x}}{\Delta} - f_3 \operatorname{erfc}(x/2\sqrt{\beta}) \\
&+ \frac{2}{3}D\Big\{-\alpha_2\chi_1 P_2\Big[\frac{1}{2}e^{(x^2/4\beta)}\Big(Q\Big(\alpha_2\sqrt{\beta}+\frac{x}{2\sqrt{\beta}}\Big) + h(x-2\alpha_2\beta)Q\Big(\Big|\alpha_2\sqrt{\beta}-\frac{x}{2\sqrt{\beta}}\Big|\Big)\Big) \\
&- H(x-2\alpha_2\beta)\,e^{\beta\alpha_2^2-\alpha_2 x}\Big] + \alpha_1\chi_2 P_1\Big[\frac{1}{2}e^{-(x^2/4\beta)}\Big(Q\Big(\alpha_1\sqrt{\beta}+\frac{x}{2\sqrt{\beta}}\Big) \\
&+ h(x-2\alpha_1\beta)Q\Big(\Big|\alpha_1\sqrt{\beta}-\frac{x}{2\sqrt{\beta}}\Big|\Big)\Big) - H(x-2\alpha_1\beta)\,e^{\beta\alpha_1^2-\alpha_1 x}\Big] \\
&+ \frac{B}{\Delta}\Big(\alpha_1 P_1 M_2 e^{-\alpha_1 x} - \alpha_2 P_2 M_1 e^{-\alpha_2 x}\Big)\Big\}
\end{aligned}$$

$$\begin{aligned}
\frac{1}{A}s_t(x,\beta) &= \frac{5}{3}\frac{f_3}{\Delta}\Big(\alpha_2^2 L_1 e^{-\alpha_2 x} - \alpha_1^2 L_2 e^{-\alpha_1 x}\Big) - \frac{1}{6}\frac{f_3}{\sqrt{\pi\beta}}e^{-(x^2/4\beta)} \\
&+ \frac{2}{3}f_2 D\Big\{\alpha_2^2\chi_1\Big[\frac{1}{2}e^{-(x^2/4\beta)}\Big(Q\Big(\alpha_2\sqrt{\beta}+\frac{x}{2\sqrt{\beta}}\Big) - h(x-2\alpha_2\beta)Q\Big(\Big|\alpha_2\sqrt{\beta}-\frac{x}{2\sqrt{\beta}}\Big|\Big)\Big) \\
&+ H(x-2\alpha_2\beta)\,e^{\beta\alpha_2^2-\alpha_2 x}\Big] - \alpha_1^2\chi_2\Big[\frac{1}{2}e^{-(x^2/4\beta)}\Big(Q\Big(\alpha_1\sqrt{\beta}+\frac{x}{2\sqrt{\beta}}\Big) \\
&- h(x-2\alpha_1\beta)Q\Big(\Big|\alpha_1\sqrt{\beta}-\frac{x}{2\sqrt{\beta}}\Big|\Big)\Big) + H(x-2\alpha_1\beta)\,e^{\beta\alpha_1^2-\alpha_1 x}\Big] \\
&+ \frac{B}{\Delta}\Big(\alpha_1^2 M_2 e^{-\alpha_1 x} - \alpha_2^2 M_1 e^{-\alpha_2 x}\Big)\Big\}.
\end{aligned} \tag{18}$$

In (18)

$$H(\xi) = \begin{cases} 0 & \xi<0 \\ 1 & \xi\geq 0 \end{cases} \qquad h(\xi) = \begin{cases} -1 & \xi<0 \\ 1 & \xi>0 \end{cases}$$

and

$$\Delta = L_1 M_2 - L_2 M_1, \quad B = \chi_2 L_1 Q(\alpha_1\sqrt{\beta}) - \chi_1 L_2 Q(\alpha_2\sqrt{\beta}).$$

As $t\to\infty$ the "fully saturated" elastic solution, obtained by taking limits of (18) as $\beta\to\infty$, reads

$$\begin{aligned}
\frac{1}{A}s_n(x,\infty) &= -f_3\Big[1+\frac{5}{3}\frac{1}{f_2\Delta}(\alpha_1 P_1 L_2 e^{-\alpha_1 x} - \alpha_2 P_2 L_1 e^{-\alpha_2 x})\Big] \\
\frac{1}{A}s_t(x,\infty) &= -\frac{5}{3}\frac{f_3}{\Delta}(\alpha_1^2 L_2 e^{-\alpha_1 x} - \alpha_2^2 L_1 e^{-\alpha_2 x}).
\end{aligned} \tag{19}$$

‡The numerical value of a_j $(j=1,2,\ldots 5)$ and p are given in Section 7.1.26, on page 299 of Ref.[7]. This approximation is valid for all z.

4. VISCOELASTIC SOLUTION FOR MOISTURE DIFFUSION UNDER CONSTANT AMBIENT HUMIDITY

Uniaxial-tension experiments[8] on epoxy indicate that its creep-response can be described by a "power law" form as follows:

$$D(t;T) = D_0(T) + D_1\left[\frac{t}{a(T)}\right]^q. \tag{20}$$

In (20) T denotes temperature and $a(T)$ is the "shift-factor" function. Additional data on polyester[9] and epoxy[10] indicate that the creep-response depends also on the moisture content m, namely $D = D(t;T,m)$. However, this dependence is omitted in the present analysis. Furthermore, we shall consider the case of uniform temperature for the entire adhesive.

In most adhesives the Poisson's ratio ν remains constant under a wide range of conditions. Consequently we shall consider a viscoelastic shear-compliance of the form

$$\mu(t) = d_0(1 + d_1 t^q)$$

where

$$d_0 = 2(1+\nu)\,D_0.\dagger \tag{21}$$

Denote $\tau = a^2/k$ and $\tau_r = d_1^{-1/q}$. Let p be the variable of the Laplace transform in the time domain and $\eta = p\tau$. Finally, let the ratio between the characteristic diffusion time τ and the characteristic creep time τ_r be $\theta = \tau_r/\tau$.

Then, the Laplace-transform of (21) is

$$\frac{1}{d_0}\,p\bar{D}(p) = 1 + \frac{\Gamma(q+1)}{(\theta\eta)^q}. \tag{22}$$

The reciprocity relations between the transforms of the creep and relaxation functions[11] yield

$$d_0 p\bar{E}(p) = 1/[1 + \Gamma(q+1)/(\theta\eta)^q] = R(\theta\eta). \tag{23}$$

Upon insertion of the explicit expressions for A_1 and A_2 into (16), the Laplace transforms of the elastic stresses (denoted by $\hat{s}$) become

$$\begin{aligned}
\frac{1}{A}\,p\hat{s}_n(x,p) = {} & \frac{2}{3}D\Bigg[\eta\left(\frac{\alpha_1\chi_2 P_1}{\sqrt{\eta}+\alpha_1}\cdot\frac{e^{-\sqrt{\eta}x}-e^{-\alpha_1 x}}{\sqrt{\eta}-\alpha_1} - \frac{\alpha_2\chi_1 P_2}{\sqrt{\eta}+\alpha_2}\cdot\frac{e^{-\sqrt{\eta}x}-e^{-\alpha_2 x}}{\sqrt{\eta}-\alpha_2}\right) \\
& + \sqrt{\eta}\left(\frac{\chi_2 L_1}{\sqrt{\eta}+\alpha_1} - \frac{\chi_1 L_2}{\sqrt{\eta}+\alpha_2}\right)\frac{\alpha_1 P_1 M_2 e^{-\alpha_1 x} - \alpha_2 P_2 M_1 e^{-\alpha_2 x}}{\Delta}\Bigg] \\
& - f_3 e^{-\sqrt{\eta}x} + \frac{5}{3}\frac{f_3}{f_2}\frac{\alpha_2 P_2 L_1 e^{-\alpha_2 x} - \alpha_1 P_1 L_2 e^{-\alpha_1 x}}{\Delta} \\
\frac{1}{A}\,p\hat{s}_t(x,p) = {} & -\frac{f_3}{6}\sqrt{\eta}\,e^{-\sqrt{\eta}x} - \frac{5}{3}f_3\frac{L_2\alpha_1^2 e^{-\alpha_1 x} - L_1\alpha_2^2 e^{-\alpha_2 x}}{\Delta} \\
& - \frac{2}{3}f_2 D\sqrt{\eta}\Bigg[\frac{\alpha_1^2\chi_2}{\sqrt{\eta}+\alpha_1}\frac{\sqrt{\eta}\,e^{-\alpha_1 x} - \alpha_1 e^{-\sqrt{\eta}x}}{\sqrt{\eta}-\alpha_1} - \frac{\alpha_2^2\chi_1}{\sqrt{\eta}+\alpha_2}\frac{\sqrt{\eta}\,e^{-\alpha_2 x} - \alpha_2 e^{-\sqrt{\eta}x}}{\sqrt{\eta}-\alpha_2} \\
& + \left(\frac{\chi_2 L_1}{\sqrt{\eta}+\alpha_1} - \frac{\chi_1 L_2}{\sqrt{\eta}+\alpha_2}\right)\frac{\alpha_2^2 M_1 e^{-\alpha_2 x} - \alpha_1^2 M_2 e^{-\alpha_1 x}}{\Delta}\Bigg].
\end{aligned} \tag{24}$$

Note that the singularities at $\sqrt{\eta} = \alpha_1$ and $\sqrt{\eta} = \alpha_2$ are removable.

†The non-dimensional viscoelastic stresses are given by $s_{ij} = \sigma_{ij}/d_0$.

From the fundamental equations of linear viscoelasticity[12] it follows that the Laplace transforms of the viscoelastic solution to our problem (denoted by overbars) are

$$\frac{d_0}{A} p\bar{s}_n(x, p) = R(\theta\eta) \cdot \frac{1}{A} p\hat{s}_n(x, p)$$
$$\frac{d_0}{A} p\bar{s}_t(x, p) = R(\theta\eta) \cdot \frac{1}{A} p\hat{s}_t(x, p). \tag{25}$$

In order to obtain the viscoelastic solution in the real-time domain it is necessary to invert (25). The inversion was obtained by the method of collocation[13]. Typically, expressions (25) were plotted vs $\log \eta$ and a set on N points $\eta_i (i = 1, \ldots N)$ was selected to cover the ranges where those plots show noticeable curvatures. It was found that the shapes of the above mentioned plots, as well as the locations of high curvature regions, depended on x. Therefore, it was impossible to employ any specific set of points η_i in the inversion and an appropriate selection had to be made for each value of x.

The calculations followed the scheme of Ref.[13]. Note, however, that for a "power-law" creep as given in (20) we have $\lim_{t\to\infty} D(t, T) \to \infty$, hence the equilibrium stress vanishes. Furthermore, in the present case the transform-variable is $\eta = p\tau$, whereby the inversion is obtained in terms of dimensionless time t/τ, rather than real time t.

Calculations were performed for an adhesive-layer with the following selected properties:

Thickness $a = 0.003''$, moisture diffusivity $k = 0.2 \times 10^{-8}$ in^2/sec, Poisson's ratio $\nu = 0.45$, 100% R. H.-to-swelling conversion-factor $A = 0.03$, creep compliances $D_0 = 2 \times 10^{-6}$ in^2/lb, $D_1 = 0.2 \times 10^{-6}$ in^2/lb with $q = 0.19$. The corresponding value of the shift-factor function was $a(T) = 1$.

With the above numerical values we obtain $\tau = 4500\,\text{sec}^{-1}$ and the value of θ in (22) is $\theta = 2450$.

Numerical evaluations were performed on an Amdahl 470 digital computer. The results are shown in Figs. 2–9. The heavy solid lines in Figs. 2–7 show the dependence of the non-dimensional viscoelastic normal and tangential interlaminar stresses s_n and s_t on time t at three fixed stations within the layer, $x = X/a = 0.01$, 1 and 3, when the free edge ($x = 0$) is exposed to a constant R.H. = 100% at $t = 0$. Note that the time scale is logarithmic.

For comparison purposes, the elastic stresses—as given in (18)—are shown in thin solid lines in Figs. 2–7. Note that any station within the layer senses the build-up and approach of the

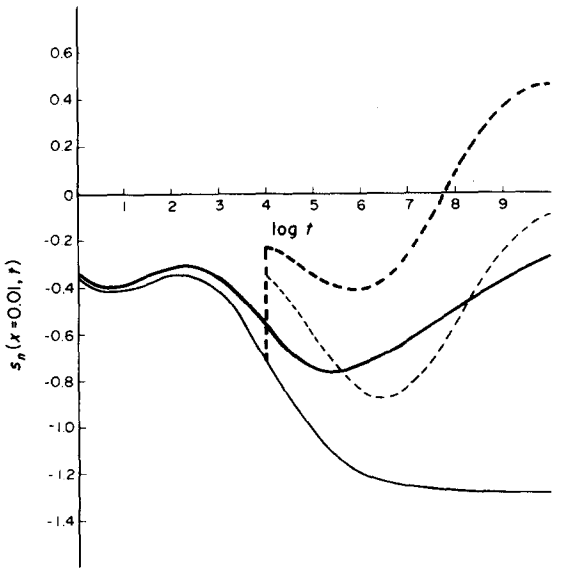

Fig. 2. Elastic and viscoelastic values of the non-dimensional normal interlaminar traction s_n at $x = X/a = 0.01$ vs. $\log t$ (t in seconds). Heavy lines—viscoelastic, thin lines—elastic. Solid lines—exposure to a constant ambient R.H., dashed lines—exposure to fluctuating ambient R.H. (according to eqn 29).

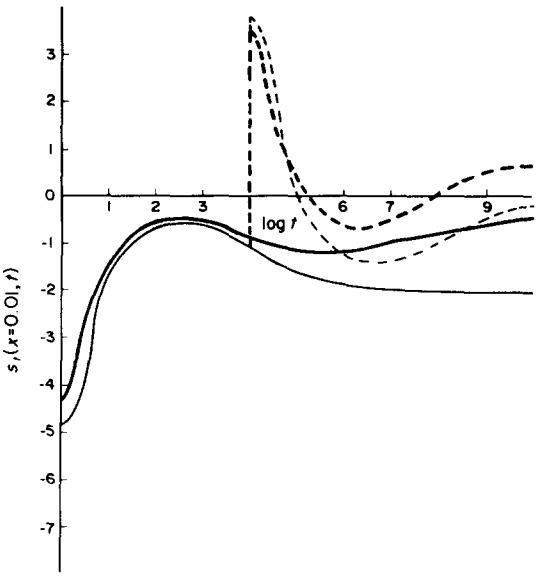

Fig. 3. Elastic and viscoelastic values of the non-dimensional tangential interlaminar traction s_t at $x = X/a = 0.01$ vs. $\log t$ (t in seconds). Heavy lines—viscoelastic, thin lines—elastic. Solid lines—exposure to a constant ambient R.H., dashed lines—exposure to fluctuating ambient R.H. (according to eqn 29).

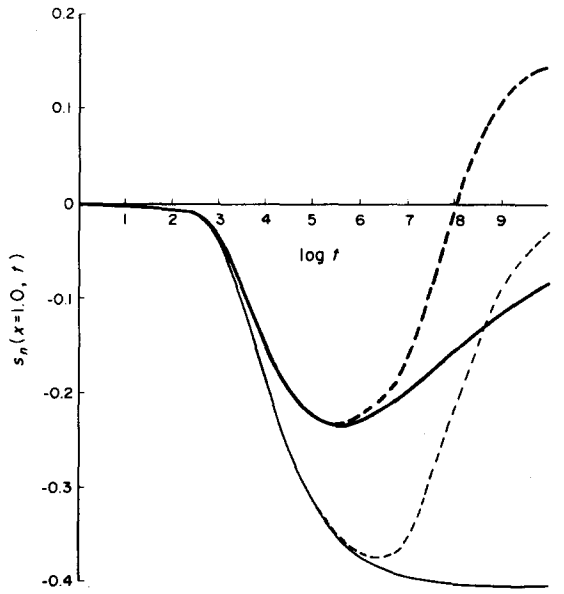

Fig. 4. Elastic and viscoelastic values of the non-dimensional normal interlaminar traction s_n at $x = X/a = 1$ vs $\log t$ (t in seconds). Heavy lines—viscoelastic, thin lines—elastic. Solid lines—exposure to a constant ambient R.H., dashed lines—exposure to fluctuating ambient R.H. (according to eqn 29).

moisture in a gradual manner and that a steep increase in stress occurs after the passage of a time-span, which depends on the characteristic diffusion time and the location of the station. Beyond that time the station notices a "fully saturated" state, which explains the leveling-off of the elastic stresses for longer times.

The viscoelastic values, which are affected by relaxation, diminish to zero with time.

Thus far all viscoelastic results were obtained from inversion of (25) by means of collocation.

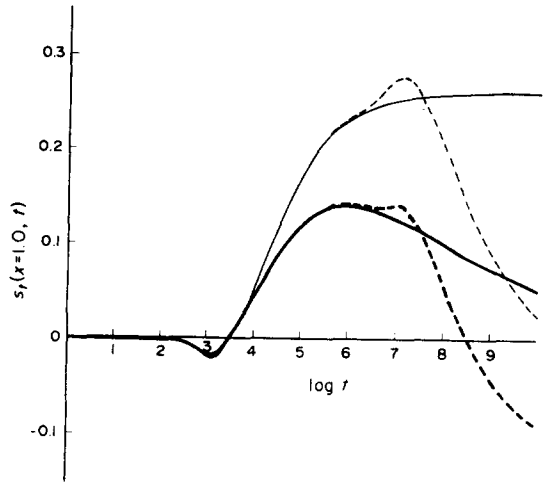

Fig. 5. Elastic and viscoelastic values of the non-dimensional tangential interlaminar traction s_t at $x = X/a = 1$ vs $\log t$ (t in seconds). Heavy lines—viscoelastic, thin lines—elastic. Solid lines—exposure to a constant ambient R.H., dashed lines—exposure to fluctuating ambient R.H. (according eo eqn 29).

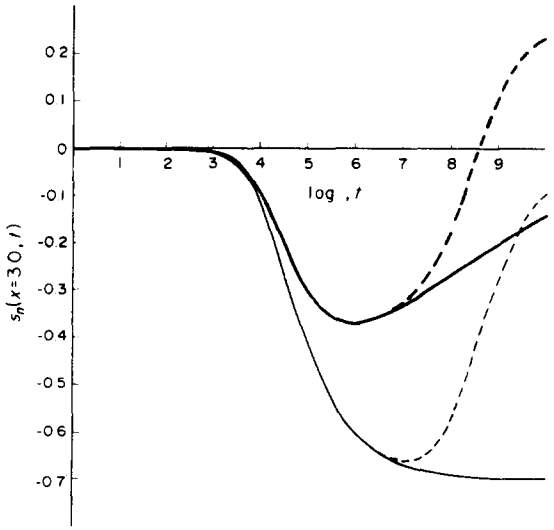

Fig. 6. Elastic and viscoelastic values of the non-dimensional normal interlaminar traction s_n at $x = X/a = 3$ vs $\log t$ (t in seconds). Heavy lines—viscoelastic, thin lines—elastic. Solid lines—exposure to a constant ambient R.H., dashed lines—exposure to fluctuating ambient R.H. (according to eqn 29).

Consider now an approximate expression for the relaxation modulus[14]

$$E(t) = \frac{1}{D(t)} \frac{\sin \pi n}{\pi n} \tag{26}$$

where

$$n = n(t) = \frac{d}{d \log t} D(t).$$

Employing (26), the "quasi-elastic" (viscoelastic) solution is given by[13]

$$\begin{aligned} s_n^{v.e.}(x, t) &= F(t) s_n(x, t) \\ s_t^{v.e.}(x, t) &= F(t) s_t(x, t) \end{aligned} \tag{27}$$

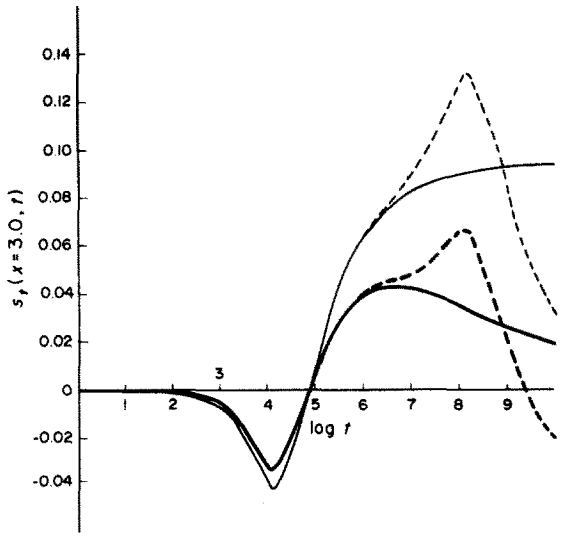

Fig. 7. Elastic and viscoelastic values of the non-dimensional tangential interlaminar traction s_t at $x = X/a = 3$ vs $\log t$ (t in seconds). Heavy lines—viscoelastic, thin lines—elastic. Solid lines—exposure to a constant ambient R.H., dashed lines—exposure to fluctuating ambient R.H. (according to eqn 29).

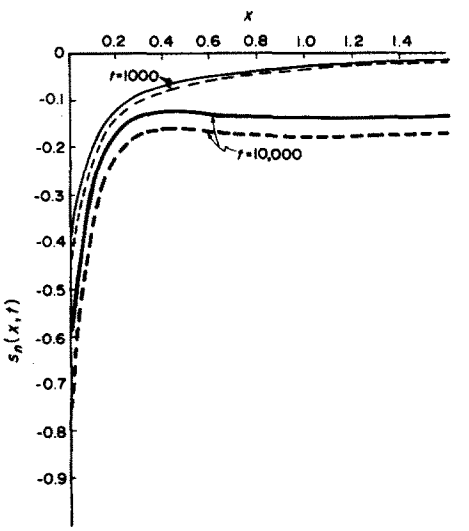

Fig. 8. Elastic and viscoelastic values of the non-dimensional normal interlaminar traction s_n at times $t = 1000$ sec and $t = 10{,}000$ sec vs x. Dashed lines—elastic, solid lines—viscoelastic.

where, in (27), $s_n(x, t)$ and $s_t(x, t)$ and the elastic expressions given in (18) and

$$F(t) = \frac{1}{1 + bt^q} \frac{\sin \pi n(t)}{\pi n(t)}$$

$$n(t) = qbt^q/(1 + bt^q)$$

with $b = 0.046$ and $q = 0.19$.

It is interesting to note that for the particular geometric and physical values for the adhesive-layer employed in the present problem the quasi-elastic approach yielded results which were almost indistinguishable from the collocated inversion. This fortuitous circumstance could not be anticipated *a priori* because the transformed expressions, (24) and (25), do exhibit large curvatures in the η domain. In general, the usefulness of a quasi-elastic method must be verified in such circumstances. In the present case expressions (27) are certainly easier to evaluate than (25).

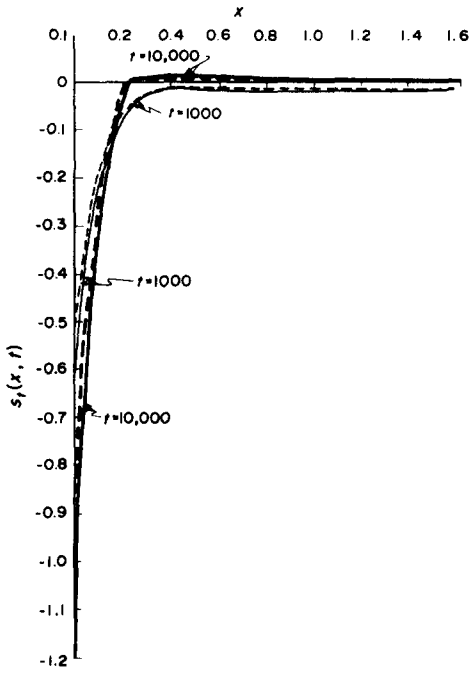

Fig. 9. Elastic and viscoelastic values of the non-dimensional tangential interlaminar traction s_t at times $t = 1000$ sec and $t = 10{,}000$ sec vs x. Dashed lines—elastic, solid lines—viscoelastic.

Employing (27), values of $s_n^{v.e.}(x, t)$ and $s_t^{v.e.}(x, t)$ were calculated for fixed values of time, $t = 1000$ sec and 10,000 sec, along the interface between the adhesive and adherend. These results are shown in Figs. 8 and 9 for $0 \leq x \leq 1.6$. (For comparison purposes, the elastic values are also shown in dashed lines.)

5. VISCOELASTIC SOLUTION UNDER FLUCTUATING AMBIENT HUMIDITY

Thus far the adhesive-layer was considered to be subjected to a sudden exposure to ambient humidity at time $t = 0$, with a swelling conversion factor A.

For fluctuating ambient humidity $A = A(t)$ the interlaminar stresses are given by a superposition integral as follows

$$s_m^{v.e.}(x, t) = \int_0^t s_m^{v.e.}(x, t - t') \frac{\mathrm{d}A(t')}{\mathrm{d}t'} \mathrm{d}t' \tag{28}$$

where $m = n$ or t.

In (28) the kernel functions, under the integral sign, are given by (27).

A sample computation was performed for a sudden exposure to 100% R.H. followed by drying at time $t = t_1$ later. In this case

$$A(t) = A[H(t) - H(t - t_1)] \tag{29}$$

whereby

$$s_m^{v.e.}(x, t) = s_m^{v.e.}(x, t) - s_m^{v.e.}(x, t - t_1) \qquad (m = n \text{ or } t). \tag{30}$$

Results for $t_1 = 10{,}000$ sec. at $x = 0.01$, $x = 1.0$ and $x = 3.0$ are shown by the dashed lines in Figs. 2–7. Note that the superposition of wetting and subsequent drying is algebraically additive in the elastic case. Therefore, all the elastic stresses, represented by thin dashed lines in Figs. 2–7, tend to zero as $t \to \infty$ *without any further sign changes.*† However, in the viscoelastic case,

†There is nevertheless an exception in Fig. 3.

the drying effects are superimposed on a *relaxed* wet state and this causes an overcompensation—thereby introducing sign-reversals in the stresses. Eventually, as $t \to \infty$, the viscoelastic stresses too tend to zero.

It is observed that viscoelasticity predicts detrimental effects that are caused by fluctuations in relative humidity—such as low cycle fatigue and interfacial tension—that are absent in an elastic analysis.

6. CONCLUDING REMARKS

The present analysis is based on several idealizations which restrict the validity of the results. The exceedingly large stresses which are predicted by linear theories near the corners $X = 0$, $Y = \pm a$ cannot be borne by real adhesives and the response in those regions must be represented by a suitable non-linear model.

In addition, the actual viscoelastic response of resins depends on the moisture content, which introduces yet another non-linearity into the analysis of adhesive layers.

The evaluation of those non-linear effects still awaits an appropriate characterization at the present time. Once available it would require solution by means of numerical methods.

Acknowledgements—The author wishes to thank Professor R. A. Schapery for many valuable discussions and Dr. S. B. Raju for his assistance in obtaining the numerical results presented herein. The author is greatly indebted to Messrs. J. E. Halkias and E. L. McKague of General Dynamics Corporation, Fort Worth, Texas for much of the information concerning the response of resins to moisture.

This work was conducted under Contract F-49620-78C-0034 from the Air Force Office of Scientific Research (AFOSR).

REFERENCES

1. Y. Weitsman, Stresses in adhesive joints due to moisture and temperature. *J. Comp. Matls* **11**, 378–394 (1977).
2. C. D. Shirrell, Diffusion of water vapor in graphite/epoxy composites. A privately communicated Air Force Materials Laboratory manuscript.
3. C-H. Shen and G. S. Springer, Moisture absorption and desorption of composite materials. *J. Comp. Matls* **10**, 2–20 (1976).
4. E. L. McKague, Jr., J. E. Halkias and I. D. Reynolds, Moisture in composites: The effect of supersonic service on diffusion. *J. Comp. Matls* **9**, 1–9 (1975).
5. I. S. Gradshteyn and I. W. Ryzhik, *Table of Integrals, Series and Products*, p. 307. Academic Press, New York (1965).
6. A. Erdelyi, W. Magnus, F. Oberhettinger and F. G. Tricomi, *Tables of Integral Transforms*, Vol. I. McGraw-Hill, New York (1954).
7. *Handbook of Mathematical Functions* (Edited by M. Abramowitz and I. A. Stegun). National Bureau of Standards (1964).
8. S. W. Beckwith, Viscoelastic characterization of a nonlinear glass/epoxy composite, including the effect of damage. Ph. D. Dissertation, Texas A&M University, (1974).
9. R. D. Maximov, Ye. A. Sokolov and V. P. Mochalov, Effect of temperature and humidity on creep of Polymeric materials. *Mechanica Polimerov* **3**, 393–399 (1975) (In Russian).
10. F. W. Crossman, R. E. Mauri and W. J. Warren, Moisture Altered Viscoelastic Response of Graphite-Epoxy Composites. Lockheed Palo Alto Research Laboratory Report. *Symp. Environmental Effects on Advanced Comp. Matls.*, sponsorred by ASTM D30 Committee, Dayton, Ohio (1977).
11. Y. C. Fung, *Foundations of Solid Mechanics*, p. 417. Prentice-Hall, New Jersey (1965).
12. Y. C. Fung, *Foundations of Solid Mechanics*, p. 414. Prentice-Hall, New Jersey (1965).
13. R. A. Schapery, Stress analysis of viscoelastic materials. *J. Comp. Matls* **1**, 228–266 (1967); especially pp. 246–247.
14. J. D. Ferry, *Viscoelastic Properties of Polymers*, p. 77. Wiley, New York (1961).